RSC Advances

PAPER

View Article Online
View Journal | View Issue

Check for updates

Cite this: *RSC Adv.*, 2024, **14**, 26115

Effect of deuterium content on the structural, optical, and thermal properties of DKDP crystals: a systematic analysis

Guodong Lei,[ab] Lisong Zhang,[ab] Mingxia Xu,[ab] Baoan Liu*[ab] and Xun Sun*[ab]

Deuterated potassium dihydrogen phosphate (DKDP) crystals with different deuterium contents have a wide range of applications, such as frequency conversion in high power lasers, electro-optic modulation, and Q-switching crystals for Pockels cells. However, there is a lack of systematic research on the effect of deuterium content on the fundamental structure and properties of these DKDP crystals. To this end, in this study, a series of DKDP crystals with different deuterium contents have been grown using the "point-seed" rapid growth method, and the structure and properties of the crystals have been characterized. The results indicate that as the deuterium content increases, the cell parameter along the *a*(*b*)-axis direction gradually increases, and the transmittance gradually increases in the infrared range. A small amount of doping (low H or D ratio) reduces the structural integrity of the crystal, and the crystals at intermediate deuterium concentrations have better crystallinity. The thermal properties of the crystals do no change significantly with the variation in the deuterium content. Overall, these findings can serve as a useful reference for boosting the application of DKDP crystals with various deuterium contents.

Received 1st July 2024
Accepted 5th August 2024

DOI: 10.1039/d4ra04776a

rsc.li/rsc-advances

Open Access Article. Published on 19 August 2024. Downloaded on 8/29/2025 7:26:52 PM.
This article is licensed under a Creative Commons Attribution-NonCommercial 3.0 Unported Licence.

1 Introduction

Deuterated potassium dihydrogen phosphate [$K(D_xH_{1-x})_2PO_4$, DKDP] is an isotopic compound formed by replacing the H atom with a D atom in potassium dihydrogen phosphate (KH_2PO_4, KDP). It is a high-performance multifunctional crystal material. Owing to its remarkable properties, such as a wide transmittance band, low half-wave voltage, large linear electro-optic coefficient, excellent optical uniformity, and ability to grow into large-sized crystals, DKDP crystals have been some of the most commonly used crystal materials in both nonlinear optics and electro-optic applications since the 1960s.[1–4]

At present, DKDP crystals are extensively applied in high-power laser facilities for inertial confinement fusion (ICF) and high-power optical parametric chirped pulse amplification (OPCPA) technology. DKDP crystals with different degrees of deuteration play diverse roles in different devices. In ICF engineering, DKDP crystals are mainly used as frequency doubling converters[5] and electro-optic switches.[6] The retracing point of DKDP crystals with deuterium content of 12% has been calculated[7] to be approximately 1.05 μm, which can be used as a frequency conversion crystals for a 1.05 μm laser with a bandwidth greater than 20 nm. At the National Ignition Facility (NIF) in the USA, DKDP crystals with a deuterium content of 70% are primarily used for third-harmonic generation,[8] and in the Laser Inertial Fusion Energy (LIFE) program, Z-cut DKDP crystals with a deuterium content of 98% are used as Pockels cells.[8] The gradient deuterium DKDP crystals grown by continuously changing the deuterium content allow the possibility of group velocity matching and an effective conversion process for third-order harmonic generation in broadband lasers.[9] At the same time, DKDP crystals can be used as frequency converters for fourth- and fifth-harmonic generation,[10,11] facilitating the design of deep ultraviolet lasers.[12] In OPCPA technology, DKDP crystals with different deuteration levels play a key role.[13] Over the past few decades, OPCPA based on DKDP crystals with a deuterium content of 88.7% has been widely explored for the development of ultra-intense femtosecond laser systems.[14] Several researchers have proposed that tens PW superintense lasers can be generated by large aperture DKDP-based OPCPA with bandwidth around 200 nm near the center wavelength of 910 or 925 nm, using DKDP crystals with deuterium content above 90%.[15] Besides, the OPCPA system based on DKDP crystal (with a deuterium content of 58.3%) and pumped by 10 kJ level Nd:glass laser has emerged as an effective way to develop 100 PW pulsed lasers with pulse duration below 20 fs.[16–18] By adjusting the deuteration level of DKDP crystals (with deuterium content of 70% and 98%) to change their phase matching characteristics, they can offer a wider range of applications in OPCPA.[19] In addition, S. B. Bodrov *et al.* experimentally validated the potential of DKDP crystals as terahertz wave generators.[20]

[a]*State Key Laboratory of Crystal Materials, Shandong University, Jinan 250100, China. E-mail: baliu@sdu.edu.cn; sunxun@sdu.edu.cn*

[b]*Key Laboratory of Functional Crystal Materials and Device, Ministry of Education, Shandong University, Jinan 250100, China*

© 2024 The Author(s). Published by the Royal Society of Chemistry

Open Access Article. Published on 19 August 2024. Downloaded on 8/29/2025 7:26:52 PM. This article is licensed under a Creative Commons Attribution-NonCommercial 3.0 Unported Licence.

The properties of crystal materials are mainly governed by their chemical composition and crystal structure, and the higher electro-optic coefficient and weaker transverse stimulated Raman scattering (TSRS) in DKDP crystals compared to KDP crystals[21,22] is closely related to the changes in the crystal structure after deuteration. The homogeneity of the structure is a crucial factor affecting the physical properties of crystals.[23] The inhomogeneity of the structure can change the phase-matching conditions, which may lead to spatial variations in the fluence distribution of non-homogeneous output waves or spatial variations in their temporal or spectral properties in the case of broadband sources. These variations have a detrimental impact on the output energy and beam quality for all the waves as well as on the temporal recompression of broadband waves in OPCPA systems,[24] and in severe cases, they may cause crystal damage. Crystal transmittance is an important parameter for characterizing the crystal performance, and the high transmittance from near-infrared to ultraviolet bands is the foundation of applying DKDP crystals as frequency conversion devices. All these parameters affect the application of DKDP crystals in different fields. Xu *et al.* investigated various properties of DKDP crystals with deuterium content of 55%, 65% and 70%.[25,26] Wang *et al.* have studied the nonlinear optical properties of DKDP crystals with a deuterium content of 12%, 70% and 80%.[27] However, the effects of partial substitution of H atoms by D atoms on the integrity and properties of DKDP crystals have not been systematically analyzed yet.

With the growing application scope of DKDP crystals, it is of immense significance to examine the effect of deuterium content on the crystal properties. To this end, in this work, a series of DKDP crystals with different deuterium contents have been grown using the "point-seed" rapid growth method, and the structural integrity, transmittance, and thermal properties of the grown crystals are comprehensively investigated, which can provide reference for advancing the application of DKDP crystals with different deuterium contents.

2 Experiments

2.1 Crystal growth

A solution with a 90% deuteration content was first prepared, and the saturation temperature of the solution was set to 45 °C. After the crystals were grown, the remaining solution was used to reduce the deuterium content by adding high-purity water and KDP raw material, while the saturation point of the solution was increased to 45 °C. A series of crystals with different deuterium contents were sequentially grown, with the lowest deuterium content being 17%. The crystal growth solution with zero deuterium content was reconfigured using KDP raw material and high-purity water. The solution was filtered through a 0.22 μm membrane.

The DKDP crystal was grown by using the point-seed rapid growth method in a 5000 ml glass bottle. The seed crystal was a Z-cut cylindrical KDP crystal, whose diameter and height were approximately 6 mm, and the growth direction was vertical. After cleaning the seed crystal, it was sealed with a special protection device and heated for 24 h, with the growth solution at 20 °C above the saturation point. Subsequently, it was cooled to 2 °C above the saturation point of the solution to remove the protection device and then naturally cooled to 0.5–0.8 °C below the saturation temperature to restore the crystal growth. Next, based on the solubility curve of DKDP and the set growth rate, the cooling curve was used to achieve rapid growth of DKDP crystals under high supersaturation. In all the experiments, FP21 program was adopted to automatically control the water bath temperature, with the temperature control accuracy of ±0.1 °C. The seed crystal rotated in the "positive-reverse-positive" mode with a speed of 77 rpm. The same growth method was used to grow KDP crystals under similar growth conditions.

2.2 Inductively coupled plasma mass spectrometry

To ensure the reliability of the experiment, it is necessary to analyze the impurity ion content in the growth solution and the grown crystal. Thus, inductively coupled plasma mass spectrometry (ICP-MS; Thermo Fisher X2) was used to detect the content of impurity metal ions in the raw material and crystals.

2.3 X-ray diffraction

Single crystal X-ray diffraction (SCXRD) measurements were conducted on a Bruker D8 three-circle diffractometer equipped with a rotating-anode generator (Mo-Kα radiation, $\lambda = 0.71073$ Å), multi-layer optics, and an APEX-II CCD detector. The data was corrected using the multi scan method.[28]

The integrity of the crystal structure was analyzed by measuring the full width at half maximum (FWHM) of high-resolution X-ray diffraction (HRXRD) peak using a high-resolution X-ray diffractometer (D5005, Bruker-AXS, Germany) under a voltage of 40 kV and current of 35 mA.

2.4 Transmittance and thermal properties

The transmittance of the DKDP crystals was tested using a spectrometer (Hitachi U-3500) under a wavelength of 200–2000 nm. Further, the constant pressure specific heat of the DKDP crystals was measured using a differential scanning calorimeter (Mettler Toledo's DSC 822e). The thermal diffusion coefficient of crystals was measured using a laser thermal conductivity meter (NETZSCH LFA 457 MicroFlash®).

3 Results and discussion

3.1 Crystal growth

A total of 9 DKDP and KDP crystals with different deuterium contents were grown. The growth parameters of the crystals are listed in Table 1, which are basically consistent. All the crystals had a transparent appearance with no visible macroscopic defects. Fig. 1 presents the photographs of the nine crystals grown in this experiment. The crystal morphology is highly dependent on the size of the seed crystals and the size of the holes in the plate of seed crystal holder; crystals grown in the holder with larger holes have a more stumpy shape, which affects the size of the final crystal.

© 2024 The Author(s). Published by the Royal Society of Chemistry

Open Access Article. Published on 19 August 2024. Downloaded on 8/29/2025 7:26:52 PM. This article is licensed under a Creative Commons Attribution-NonCommercial 3.0 Unported Licence.

Table 1 Growth parameters of DKDP crystals with different deuteration contents[a]

No.	Crystal size (mm)	Temperature reduction range (°C)	Growth rate (mm d^{-1})		D_s (%)	D_c (%)
			a	c		
1	36 × 40 × 62	40.5–33.0	0.95	2.95	90	85
2	43 × 53 × 50	42.5–35.7	1.77	3.33	80	74
3	38 × 45 × 47	45.0–38.7	1.61	3.56	70	62
4	44 × 47 × 47	41.5–33.0	1.68	3.56	60	51
5	44 × 52 × 48	42.5–33.7	1.63	3.00	50	41
6	51 × 52 × 45	45.5–35.8	2.17	3.75	40	32
7	46 × 47 × 40	43.0–32.9	2.35	4.00	30	23
8	43 × 43 × 41	44.8–37.0	1.54	2.92	17	12
9	48 × 50 × 36	46.0–37.7	1.92	2.77	0	0

[a] D_s represents the deuterium content in the solution. Here, "X% DKDP" represents the deuterium content in the crystal, the deuterium content of these DKDP crystals (D_c) is calculated according to the deuterium segregation formula,[29] the two values of "Growth rate" refer to the growth rate of the crystal in the a-direction and c-direction, respectively.

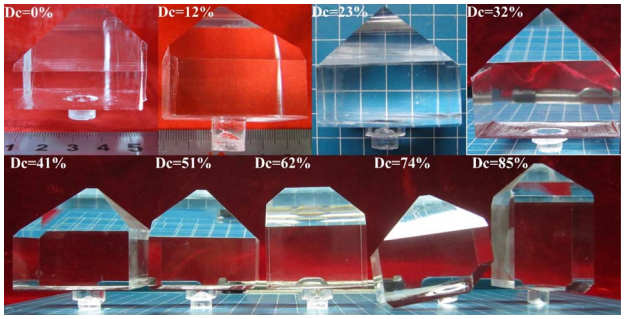

Fig. 1 Photographs of crystals with different deuteration contents grown by point seed technique. In the diagram, the blue grids represent 1 cm each.

3.2 Impurity content

The purity of the solution is the key to successful crystal growth. If the raw material contains a large number of impurities, it can directly affect the growth and quality of the crystal. At the same time, a large number of impurity ions can also affect the properties of the crystal. Imported high-purity raw materials (Merck) were used in this experiment, and the impurity metal ion content in the raw materials was measured. On the crystals obtained by rapid growth method, both pyramidal sector and prismatic sector were observed. Samples were separately prepared from the pyramidal sector and prismatic sector of the KDP crystal. All the test results of the raw materials and crystals are presented in Table 2.

For the crystals obtained by rapid growth method, the impurity metal ion content in the prismatic sector is significantly higher than that in the pyramidal sector. Due to the alternating arrangement of positively charged K^+ and negatively charged $H_2PO_4^-$ ions on the (100) surface of the crystal, with $H_2PO_4^-$ arranged on the outermost layer, the (100) surface of the crystal exhibits a negative potential.[30] It is clear that metal cations with a positive potential are preferentially adsorbed on the prismatic sector of the crystal.

Table 2 Mass content of main metallic ion impurities in the raw materials and crystals

Element (ppm)	Fe	Co	Mn	Mg	Cu	Na	Ba
Raw materials	0.105	0.003	0.042	0.022	0.023	0.421	0.021
Pyramidal sector	0.585	0.030	0.014	0.072	0.099	0.948	0.177
Prismatic sector	1.561	0.060	0.025	0.133	0.085	2.740	0.430

3.3 Crystal structure and integrity

The series of crystals prepared with different deuterium contents were cut into appropriate sizes in a glove box and pasted on top of a glass rod with AB adhesive. The data were collected at a low temperature of 150 K, and the samples were protected with Paratone oil and liquid nitrogen. The data integration and processing were carried out using the APEX2 software, while the structural analysis was conducted using the SHELXTL-97 program. Generally, the position of heavy atoms was determined using the direct or Patterson method, and the coordinates of other atoms were obtained using the difference Fourier synthesis method. All atomic coordinates and anisotropic parameters were refined to convergence using the full-matrix least-squares plane refinement method based on F2.[31] After structural convergence, all atomic positions were finally standardized using the STRICT TIDY program.[32,33] The lattice parameters of the DKDP crystals with different deuterium contents obtained from SCXRD experiments are shown in Fig. 2.

According to the Landolt–Börnstein table,[34] the O–H–O bond length in the KH_2PO_4 crystal structure at room temperature is 2.487 Å, while in the KD_2PO_4 crystal structure, the O–D–O bond length is 2.519 Å, indicating an increase in the hydrogen bond length after deuterium atom replaces hydrogen atom. It can be seen in (Fig. 3) that the cell parameter $a(b)$ value increases with the increase in deuterium content, while the c value has no obvious variation trend. This can be attributed to the fact that the O–D bond in the crystal structure is basically perpendicular to the c-axis (as shown in Fig. 3). As the deuterium content increases, the proportion of O–D in the crystal increases, so the value of $a(b)$ perpendicular to the c-axis gradually increases. The lattice constant c is primarily determined by the phosphorus–oxygen tetrahedron, so its variation is small.

Open Access Article. Published on 19 August 2024. Downloaded on 8/29/2025 7:26:52 PM.
This article is licensed under a Creative Commons Attribution-NonCommercial 3.0 Unported Licence.

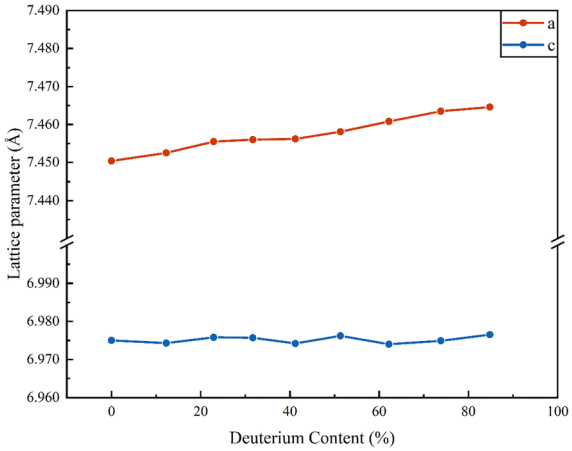

Fig. 2 Variation in the unit cell parameters with the deuterium contents.

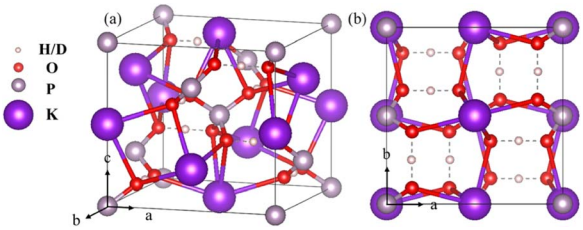

Fig. 3 Single cell structure of deuterated KDP crystals (a) and projection along the *c*-axis (b).

The DKDP crystals prepared with different deuterium contents were oriented using an X-ray crystal orientation instrument and cut vertically in the [001] direction (*i.e.*, Z-cut) with a thickness of approximately 6 mm. After rough grinding, the blank surface was polished to an optical plane, and the crystal's rocking curve was measured. The structural integrity of the crystal was characterized by the half peak width of the rocking curve. The FWHM of the rocking curves for (004) and (200) plane of all the crystals is shown in Fig. 4.

According to Fig. 4, the half peak width of the (004) crystal plane rocking curves of these crystals is relatively large at low deuterium content (12%) and high deuterium content (74%, 85%). This indicates that the 12% DKDP crystal, 74% DKDP crystal, and 85% DKDP crystal have poorer structural integrity than the other crystals, with better integrity observed at intermediate deuterium concentrations. The crystals with low and high deuterium contents can be regarded as low deuterium-doped KDP crystals and low hydrogen-doped DKDP crystals, respectively, indicating that a small amount of doping can reduce the structural integrity of the crystals. Furthermore, Liu *et al.* demonstrated that there are variations in the homogeneity of the deuterium content in crystals with differing deuterium concentrations, which can also influence the structural integrity of the crystals.[35]

The half width of the (200) crystal plane rocking curve does not show any obvious regularity, but it is much larger than that

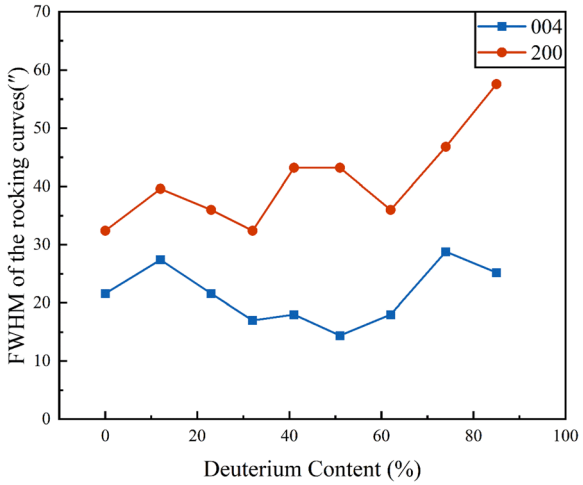

Fig. 4 FWHM of the rocking curves for (004) and (200) plane of DKDP crystals.

of the (004) crystal plane, which is related to the hydrogen bonds parallel to the [100] or [010] direction in the crystal structure. After the hydrogen atom on the hydrogen bond is replaced by deuterium atom, the bond length increases, causing lattice distortion on the crystal plane in this direction due to compressive stress.

In addition, as shown in Fig. 5, unlike the diffraction patterns of other crystals, additional peaks near the main peak of the (004) crystal plane rocking curve are found in the 12% DKDP crystal. The short-dotted line in the figure is fitted by Gaussian fitting, which is consistent with the experimental curve. The additional peak is separated by 34″ from the main peak, which is caused by the small angle grain boundaries (≤1″) within the crystal structure.[36] The orientation difference between grain boundaries and the main crystallization direction is 34″. Although the tilt angle is small, the substitution of hydrogen atom by deuterium atom and the compressive stress generated by hydrogen bond growth between atomic layers lead to the appearance of grain boundaries in the crystal.

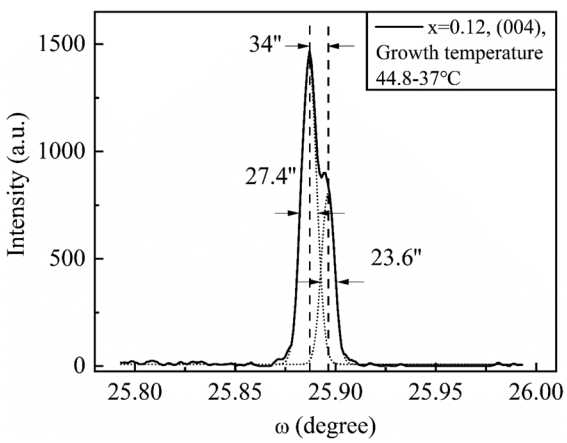

Fig. 5 Rocking curves of 12% DKDP crystal.

© 2024 The Author(s). Published by the Royal Society of Chemistry

Open Access Article. Published on 19 August 2024. Downloaded on 8/29/2025 7:26:52 PM.
This article is licensed under a Creative Commons Attribution-NonCommercial 3.0 Unported Licence.

3.4 Transmittance

Two pieces of type II third-harmonic generation slices ($\theta = 59°$, $\psi = 0°$) and Z slices ($\theta = 0°$, $\psi = 0°$) were cut from the prismatic sector of the crystal, with a sample size of 13 mm × 13 mm × 11 mm. The surface of the blank piece was first oriented (accuracy ±7′), then rough-grained and fine-grained. Finally, it was polished using traditional polishing methods with an anhydrous abrasive slurry to obtain a bright surface for testing.

Fig. 6(a) and (b) show the transmission spectra of Z-cut slice and frequency tripler-cut slice of DKDP crystals with different deuterium contents. It can be seen that with the increase in the deuterium content, the transmission spectral range of the crystal increases, and the infrared cut-off edge shifts to a longer wavelength. This difference is caused by the substitution of hydrogen atom by deuterium atom in the hydrogen bond, and the binding force of D–O bond is weaker than that of H–O bond.[37] Fig. 6(c) shows the transmission spectrum of DKDP crystal with 85% deuterium content. It can be seen that the spectrum of the frequency tripler-cut slice has an obvious red shift with respect of that of the Z-cut slice, and the transmission range is wider. In addition, the ultraviolet absorption of the crystal is slightly increased, which is due to the position of the sample in the cylindrical sector of the crystal. The cylindrical crystal absorbs a large number of metal impurities ions during the growth process due to its apparent negative potential, so the measured samples have obvious absorption peaks in the ultraviolet region. As shown in Fig. 6(d), the crystal shows obvious absorption peaks at 230 nm and 280 nm, which may be caused by the absorption of metal ions (Fe^{3+}).[38]

3.5 Thermal properties

The thermal diffusion coefficient and constant pressure specific heat of the crystal were first measured, and then the thermal conductivity was calculated using the following relationship:

$$\kappa = \lambda \cdot \rho \cdot C_p \quad (1)$$

where κ represents the thermal conductivity, λ represents the thermal diffusion coefficient, ρ represents the density, and C_p represents the specific heat at constant pressure.

The density of the DKDP crystals with different deuterium contents was tested using the buoyancy method at room temperature (test temperature: 30.2 °C), and the crystal density was calculated as follows:

$$\rho = \frac{m\rho_{water}}{m - m'} \quad (2)$$

where ρ_{water} represents the density of water at the test temperature, m represents the weight of the crystal in air, and m'

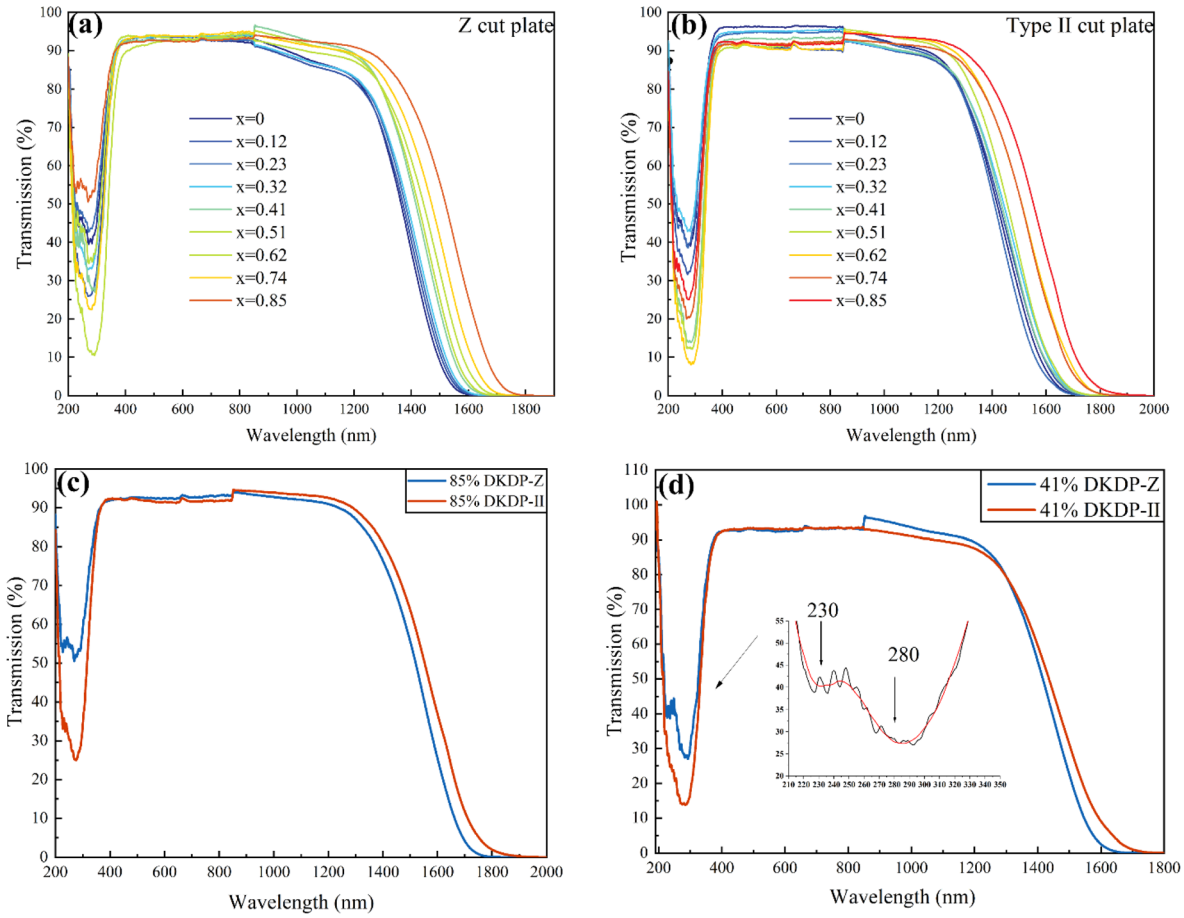

Fig. 6 Transmission spectrum of the DKDP crystal (a) Z-cut plate crystal (b) tripler-cut plate crystal (c) 85% DKDP crystal (d) 41% DKDP crystal.

Open Access Article. Published on 19 August 2024. Downloaded on 8/29/2025 7:26:52 PM.
This article is licensed under a Creative Commons Attribution-NonCommercial 3.0 Unported Licence.

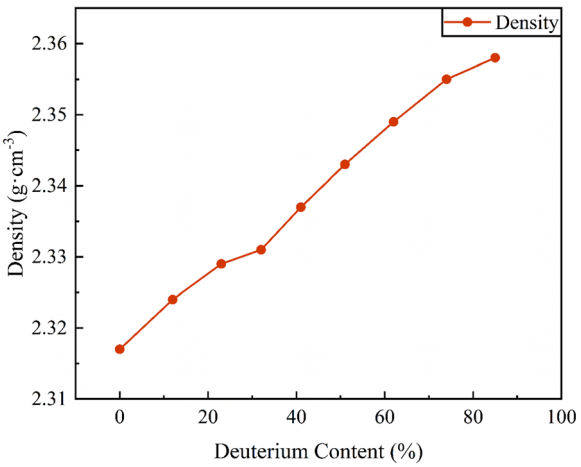

Fig. 7 Density of $K(D_xH_{1-x})_2PO_4$ crystals at 30.2 °C.

represents the weight of the crystal completely immersed in water.

The densities of the series of DKDP crystals with different deuterium contents (measured by the buoyancy method) are shown in Fig. 7. It can be seen that the density of the crystal increases with the increase in the deuterium content. This is because deuterium atoms have one more neutron in the nucleus than hydrogen atoms, with an atomic mass of 2. As deuterium replaces more hydrogen, the density of the crystal increases.

The temperature range for the constant pressure specific heat test was 25–120 °C, with a heating rate of 5 °C min^{-1} and constant pressure nitrogen protection. The sample was a block of 3 mm × 3 mm × 1 mm, with two tangential directions, *a* and *c*. From room temperature to 120 °C, the specific heat of the series of deuterium content crystals is shown in Fig. 8, and it can be seen that the specific heat of all crystals is between 0.8 and 1.3 J g^{-1} K^{-1}.

For the DKDP crystal in the tetragonal crystal system, its thermal diffusion coefficient, after being spindle oriented, only has two independent principal values λ_1 (=λ_2) and λ_3. The

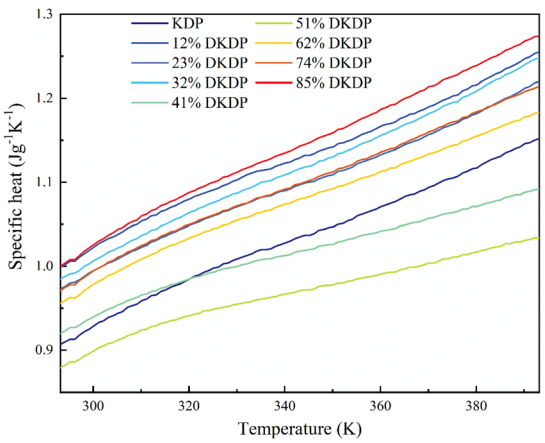

Fig. 8 Temperature dependence of the specific heat of DKDP crystals with different deuteration contents.

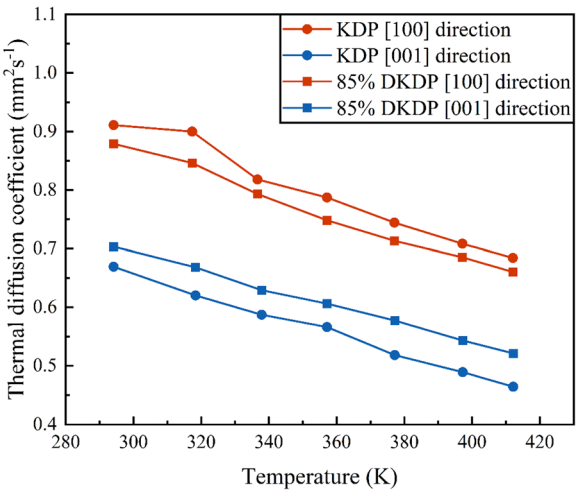

Fig. 9 Thermal diffusion coefficient of KDP crystal and 85% DKDP crystal.

thermal diffusion coefficients in the [100] direction and [001] direction of crystal crystallography can be measured separately. Samples in the [100] and [001] directions were processed separately, with sample sizes of 4 mm × 4 mm × 1 mm.

Fig. 9 shows the temperature dependent thermal diffusion coefficients of pure KDP crystals and 85% DKDP crystals. It can be seen that the thermal diffusion coefficient of the crystal decreases with the increase of temperature, and the values of the [100] direction are all greater than the [001] direction.

Based on the measured thermal diffusion coefficients of crystals with different deuterium contents and the density of these crystals previously measured by buoyancy method, the thermal conductivity of a series of deuterium content crystals were calculated using eqn (1). The thermal conductivity of crystals with different deuterium contents at room temperature is shown in Fig. 10. From the figure, it can be seen that the thermal conductivity of DKDP crystal does not show a regular change with the increase of deuterium content in the crystal. The reasons for the analysis are as follows: firstly, the quality of

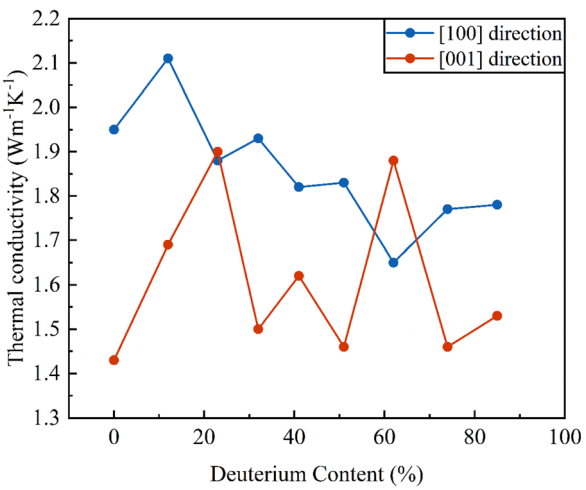

Fig. 10 Thermal conductivity of the $K(D_xH_{1-x})_2PO_4$ crystals at 30.2 °C.

© 2024 The Author(s). Published by the Royal Society of Chemistry

Open Access Article. Published on 19 August 2024. Downloaded on 8/29/2025 7:26:52 PM. This article is licensed under a Creative Commons Attribution-NonCommercial 3.0 Unported Licence.

the crystal is closely related to the growth conditions of the crystal. The DKDP crystal sample used in this experiment was obtained by rapid growth using the point seed crystal method, and there were still some conditions that were not completely consistent during the crystal growth process. Secondly, during the rapid growth process of crystals, both pyramidal sector and prismatic sector grow simultaneously. Due to the different surface structures of the two, pyramidal sector and prismatic sector with different crystal quality are finally formed in the crystal. Although the samples for the thermal diffusion experiment are taken from the pyramidal sector of the crystal, the uneven defect distribution generated in the crystal due to growth conditions still affects the thermal diffusion coefficient of the crystal. Therefore, it is not possible to clarify the influence of changes in deuterium content on the thermal diffusion coefficient and thermal conductivity of DKDP crystals, and further experimental research is needed.

4 Conclusions

In order to investigate the effect of deuterium content on crystal structure and properties, a series of DKDP crystals with different deuterium contents were grown, and their structure and properties were characterized. The cell parameter along $a(b)$ axis direction increased with the increasing of deuterium content, while the c value showed no obvious variation. This is related to the fact that the O–H(D) bonds in the crystal structure are almost perpendicular to the c-axis, and the proportion of O–D bonds in the crystal increases with the increase of deuterium content. Therefore, the lattice parameter $a(b)$ value gradually increases. The lattice constant c is mainly determined by the PO_4 tetrahedron, so its variation is small. From the rocking curve test, it was found that a small amount of doping (low H or D ratio) reduces the structural integrity of the crystal. And crystals at intermediate concentrations have better crystallinity. The half peak width of the (200) crystal plane oscillation curve did not show obvious regularity, but was much larger than that of the (004) crystal plane, which is caused by hydrogen bonds parallel to the [100] or [010] directions in the crystal structure. Due to the substitution of hydrogen by deuterium, the compressive stress generated by the growth of hydrogen bond between atomic layers may lead to the appearance of grain boundaries in the crystal.

As the deuterium content in the crystal increased, the transmittance spectrum range became wider, and the infrared part of the transmittance shifted towards longer wavelengths. This difference is mainly due to the substitution of hydrogen by deuterium in hydrogen bonds, and the binding force of D–O bonds is weaker compared to H–O bonds. The spectrum of the frequency tripler slice shows a significant redshift compared to the Z-slice, with a wider transmittance range. In the ultraviolet region, the crystal exhibited significant absorption peaks at 230 nm and 280 nm, which may be due to the absorption of metal ions (Fe^{3+}). The thermal diffusion coefficient of crystals decreased with increasing temperature, and the values of [100] direction were all greater than the [001] direction. The unexpected defects generated in the crystal due to growth conditions also may affect the thermal parameters of the crystal, making it difficult to observe the effect of deuterium content on the thermal properties of DKDP crystals. These results provide reference for the future application of DKDP crystals with different deuterium contents.

Data availability

The original contributions presented in the study are included in the article, further inquiries can be directed to the corresponding author.

Conflicts of interest

There are no conflicts to declare.

Acknowledgements

This work is supported by the Taishan Scholars Program of Shandong Province (No. tstp20231207).

References

1 J. J. De Yoreo, A. K. Burnham and P. K. Whitman, *Int. Mater. Rev.*, 2002, **47**, 113–152.
2 J. H. Campbell, R. A. Hawley-Fedder, C. J. Stolz, J. A. Menapace, M. R. Borden, P. K. Whitman, J. Yu, M. Runkel, M. O. Riley, M. D. Feit and R. P. Hackel, *NIF optical materials and fabrication technologies: An overview*, San Jose, CA, 2004, pp. 84–101, DOI: **10.1117/12.538471**.
3 R. Hawley-Fedder, P. Geraghty, S. Locke, M. McBurney, M. Runkel, T. Suratwala, S. Thompson, P. Wegner and P. Whitman, *NIF Pockels cell and frequency conversion crystals*, San Jose, CA, 2004, pp. 121–126, DOI: **10.1117/12.538482**.
4 W. P. Mason, *Phys. Rev.*, 1946, **70**, 529–537.
5 K. I. Schaffers, C. J. Stolz, J. J. Adams, R. A. Negres and M. V. Monticelli, *Proc. SPIE*, 2023, 1272603–1272609, DOI: **10.1117/12.2684120**.
6 E. Vantilburg and P. P. Banerjee, *Proc. SPIE*, 2024, **12882**, 128820I–128829.
7 H. Y. Zhu, T. Wang, W. G. Zheng, P. Yuan, L. J. Qian and D. Y. Fan, *Opt. Express*, 2004, **12**, 2150–2155.
8 A. Bayramian, S. Aceves, T. Anklam, K. Baker, E. Bliss, C. Boley, A. Bullington, J. Caird, D. Chen, R. Deri, M. Dunne, A. Erlandson, D. Flowers, M. Henesian, J. Latkowski, K. Manes, W. Molander, E. Moses, T. Piggott, S. Powers, S. Rana, S. Rodriguez, R. Sawicki, K. Schaffers, L. Seppala, M. Spaeth, S. Sutton and S. Telford, *Fusion Sci. Technol.*, 2011, **60**, 28–48.
9 G. K. Hao, M. X. Xu, X. Sun, B. A. Liu, L. S. Zhang, H. K. Ren, J. Y. Bai and J. Y. Gao, *Cryst. Growth Des.*, 2023, **24**, 567–572.
10 X. X. Chai, S. Zhou, X. B. Wang, P. Li, B. Feng, Q. H. Zhu and L. Q. Wang, *Appl. Opt.*, 2024, **63**, 1411–1417.
11 Z. J. Cui, L. Han, C. Wang, M. Y. Sun, D. A. Liu and J. Q. Zhu, *Opt. Lett.*, 2022, **47**, 2947–2950.

© 2024 The Author(s). Published by the Royal Society of Chemistry

Open Access Article. Published on 19 August 2024. Downloaded on 8/29/2025 7:26:52 PM. This article is licensed under a Creative Commons Attribution-NonCommercial 3.0 Unported Licence.

12 Z. J. Cui, M. Y. Sun, C. Wang, B. Shen, X. Zhang, D. A. Liu and J. Q. Zhu, *AIP Adv.*, 2022, **12**, 8.
13 M. Galimberti, C. Hernandez-Gomez, I. Musgrave, I. Ross and T. Winstone, *Opt. Commun.*, 2013, **309**, 80–84.
14 V. V. Lozhkarev, G. I. Freidman, V. N. Ginzburg, E. V. Katin, E. A. Khazanov, A. V. Kirsanov, G. A. Luchinin, A. N. Mal'shakov, M. A. Martyanov, O. V. Palashov, A. K. Poteomkin, A. M. Sergeev, A. A. Shaykin and I. V. Yakovlev, *Laser Phys. Lett.*, 2007, **4**, 421–427.
15 J. Bromage, S. W. Bahk, I. A. Begishev, C. Dorrer, M. J. Guardalben, B. N. Hoffman, J. B. Oliver, R. G. Roides, E. M. Schiesser, M. J. Shoup, S. B. Webb, D. Weiner and J. D. Zuegel, *High Power Laser Sci. Eng.*, 2019, **7**, 11.
16 J. B. Hu, X. L. Wang, Y. Xu, L. H. Yu, F. X. Wu, Z. X. Zhang, X. J. Yang, P. H. Ji, P. L. Bai, X. Y. Liang, Y. X. Leng and R. X. Li, *Appl. Opt.*, 2021, **60**, 3842–3848.
17 R. Dabu, *OSA Continuum*, 2021, **4**, 1658–1668.
18 Y. X. Han, Z. Y. Li, Y. B. Zhang, F. Y. Kong, H. C. Cao, Y. X. Jin, Y. X. Leng, R. X. Li and J. D. Shao, *Nat. Commun.*, 2023, **14**, 9.
19 A. Wang, P. Xue, X. Liu, X. Wang, L. Yu, X. Liang, Y. Leng and R. Li, *Opt. Express*, 2024, **32**, 3597–3605.
20 S. B. Bodrov, N. A. Abramovsky, G. S. Paramonov, S. N. Belyaev, A. P. Prokhorov, A. N. Stepanov and M. I. Bakunov, *J. Appl. Phys.*, 2023, **134**, 7.
21 L. S. Zhang, G. W. Yu, H. L. Zhou, L. Li, M. X. Xu, B. A. Liu, S. H. Ji, L. L. Zhu, F. F. Liu and X. Sun, *J. Cryst. Growth*, 2014, **401**, 190–194.
22 X. X. Chai, F. Q. Li, S. L. Wang, B. Feng, Q. H. Zhu, B. A. Liu, X. Sun and X. G. Xu, *Acta Phys. Sin.*, 2015, **64**, 7.
23 G. Bhagavannarayana, G. C. Budakoti, K. K. Maurya and B. Kumar, *J. Cryst. Growth*, 2005, **282**, 394–401.
24 C. Dorrer, I. A. Begishev, S. W. Bahk and J. Bromage, *Opt. Mater. Express*, 2022, **12**, 3679–3695.
25 M. X. Xu, Z. P. Wang, B. A. Liu, S. H. Ji, X. Sun and X. G. Xu, *Study on the properties of the DKDP crystal with different deuterium content*, Shanghai, Peoples R. China, 2011, DOI: **10.1117/12.910477**.
26 M. X. Xu, L. S. Zhang, F. F. Liu, S. Y. Wang, Y. F. Lian, F. Wang, Z. P. Wang, X. G. Xu, X. Sun and S. T. Sun, *Cryst. Res. Technol.*, 2018, **53**, 7.
27 D. L. Wang, T. B. Li, S. L. Wang, J. Y. Wang, C. Y. Shen, J. X. Ding, W. D. Li, P. P. Huang and H. Liu, *Appl. Phys. Express*, 2017, **10**, 4.
28 S. Bruker and S. Saint, *Bruker APEX2*, Madison Wisconsin, USA, 2002.
29 G. M. Loiacono, J. F. Balascio and W. Osborne, *Appl. Phys. Lett.*, 1974, **24**, 455–456.
30 S. A. de Vries, P. Goedtkindt, S. L. Bennett, W. J. Huisman, M. J. Zwanenburg, D. M. Smilgies, J. J. De Yoreo, W. J. P. van Enckevort, P. Bennema and E. Vlieg, *Phys. Rev. Lett.*, 1998, **80**, 2229–2232.
31 G. M. Sheldrick, *Acta Crystallogr., Sect. A: Found. Adv.*, 2008, **64**, 112–122.
32 E. Parthe and L. M. Gelato, *Acta Crystallogr., Sect. A: Found. Crystallogr.*, 1984, **40**, 169–183.
33 L. M. Gelato and E. Parthe, *J. Appl. Crystallogr.*, 1987, **20**, 139–143.
34 SpringerVerlag, *Landolt-Bornstein Substance/Property Index*, Springer Group, 2002.
35 F. F. Liu, PhD thesis, Shandong University, 2017.
36 G. Bhagavannarayana and S. K. Kushwaha, *J. Appl. Crystallogr.*, 2010, **43**, 154–162.
37 A. Dyan, G. Duchateau, S. Eslava, J. L. Stehle, D. Damiani and H. Piombini, *J. Mod. Opt.*, 2009, **56**, 27–31.
38 N. Y. Garces, K. T. Stevens, L. E. Halliburton, M. Yan, N. P. Zaitseva and J. J. DeYoreo, *J. Cryst. Growth*, 2001, **225**, 435–439.

© 2024 The Author(s). Published by the Royal Society of Chemistry